HA-FGOVD: Highlighting Fine-grained Attributes via Explicit Linear Composition for Open-Vocabulary Object Detection

Yuqi Ma, Mengyin Liu, Chao Zhu, Xu-Cheng Yin, *Senior Member, IEEE,*

Abstract—Open-vocabulary object detection (OVD) models are considered to be Large Multi-modal Models (LMM), due to their extensive training data and a large number of parameters. Mainstream OVD models prioritize object coarse-grained category rather than focus on their fine-grained attributes, e.g., colors or materials, thus failed to identify objects specified with certain attributes. However, OVD models are pretrained on large-scale image-text pairs with rich attribute words, whose latent feature space can represent the global text feature as a linear composition of fine-grained attribute tokens without highlighting them. Therefore, we propose in this paper a universal and explicit approach for frozen mainstream OVD models that boosts their attribute-level detection capabilities by highlighting fine-grained attributes in explicit linear space. Firstly, a LLM is leveraged to highlight attribute words within the input text as a zero-shot prompted task. Secondly, by strategically adjusting the token masks, the text encoders of OVD models extract both global text and attribute-specific features, which are then explicitly composited as two vectors in linear space to form the new attribute-highlighted feature for detection tasks, where corresponding scalars are hand-crafted or learned to reweight both two vectors. Notably, these scalars can be seamlessly transferred among different OVD models, which proves that such an explicit linear composition is universal. Empirical evaluation on the FG-OVD dataset demonstrates that our proposed method uniformly improves fine-grained attribute-level OVD of various mainstream models and achieves new state-of-the-art performance.

Index Terms—Object detection, Fine-grained open vocabulary object detection, Vision-language model

I. INTRODUCTION

THE Open-Vocabulary Object Detection (OVD) [1] is based on [2], [3] or proposes an architecture of Large Multi-modal Models (LMM) [4], [5], characterized by its extensive training data and a large number of parameters. In contrast to classical object detectors limited to closed-set categories, OVD models detects objects further beyond the category scope of their training data [6]. Although there has been a notable emergence of researches on OVD in recent years [7]–[9], major OVD models are both learned and evaluated on mainstream datasets with the typical labels

Yuqi Ma, Mengyin Liu, Chao Zhu, and Xu-Cheng Yin are with School of Computer and Communication Engineering, University of Science and Technology Beijing, Beijing 100083, China (e-mails: yuqima@xs.ustb.edu.cn, blean@live.cn, chaozhu@ustb.edu.cn, xuchengyin@ustb.edu.cn).
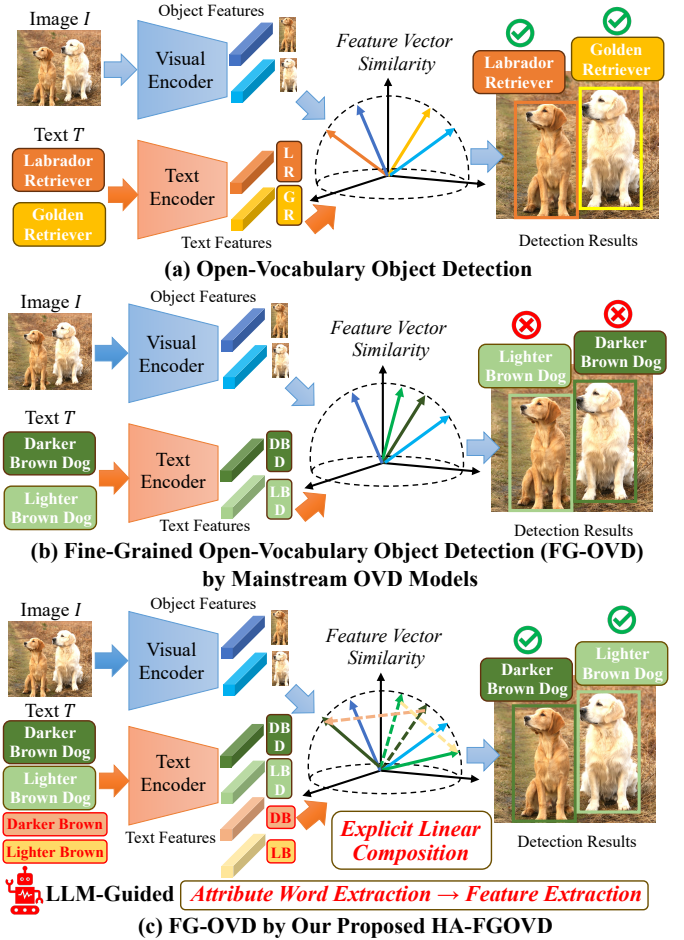Corresponding author: Chao Zhu.

Fig. 1. Difference between (a) open-vocabulary object detection for the fine-grained category names, (b) fine-grained open vocabulary object detection for the attribute-specific descriptions, and (c) our proposed HA-FGOVD method.

as only a few category names. Therefore, they struggle in following natural user instruction with a more fine-grained attribute vocabulary than category names, which requires a stronger understanding of the fine-grained semantics of the language by aligning them with visual features.

To this end, recent studies have introduced a novel task, i.e., fine-grained open-vocabulary object detection (FG-OVD) [10]. As illustrated in Fig. 1, different from traditional closed-set fine-grained object detection (FG-OD) that focuses on inter-class variations (e.g., Labrador Retriever vs Golden Retriever).

FG-OVD emphasizes extrinsic attributes (e.g., darker brown dog vs lighter brown dog) [10], which poses a challenge for OVD models. Moreover, the composition of various fine-grained attributes, e.g., color, patterns and materials, further enlarges such a fine-grained vocabulary that is not only broader than category names, but also closer to real-world application in natural language.

Meanwhile, various works on FG-OVD have researched that insufficient emphasis on attribute words during the detection training phase leads to the inability of OVD models to recognize objects with characterized attributes [10], [11]. However, OVD models, either based on or proposed as large pretrained Vision-Language Models, leverage a vast array of image-text pairs [4], [12] enriched with attribute words. These models' latent feature spaces can represent global text features as a linear composition of fine-grained attribute tokens [13], while these attributes not being specifically highlighted within the OVD model.

To address the above issues, we have proposed a universal approach that explicitly enhances the FG-OVD capabilities of OVD models by highlighting fine-grained attributes in the explicit linear space. In a plug-and-play manner for frozen mainstream OVD models, powerful Large Language Model (LLM) [14] is adopted for attribute word extraction, then text tokens are masked to guide the extraction of attribute-specific features by text encoder, which are then linearly composited with the global features for a new attribute-highlighted feature for better FG-OVD performance. The main contribution of our paper is summarized as:

1) Firstly, Attribute Word Extraction is proposed to identify attribute words within the input text as a zero-shot prompted task based on a powerful LLM.
2) Secondly, Attribute Feature Extraction strategically adjusting the token attention masks of text tokens, the text encoders of OVD models extract both global text and attribute-specific features.
3) Thirdly, we propose Attribute Feature Enhancement based on the compositional property of text embedding. Global and attribute-specific features are fused as two vectors by explicit linear composition to form the new attribute-highlighted feature for further detection.
4) Finally, experiments show the linear composition weight scalars can be learned or explicitly and seamlessly transferred among different OVD models. Evaluation on the FG-OVD dataset demonstrates that our proposed explicit and powerful approach significantly improves various mainstream OVD models and achieves new state-of-the-art performance.

II. RELATED WORKS

A. Open Vocabulary Object Detection

The task of OVD is designed to leverage rich vision-language semantics to detect objects of unseen categories during training. Hence, large vision-language models are pretrained on large-scale image-text datasets with a rich vocabulary base. For instance, CLIP [12], which was trained on 400 million (image, text) pairs, has demonstrated significant potential in learning representations that are transferable to OVD models [15] in various ways, including knowledge distillation [16], [17], serving as an encoder for visual or textual data [3], [18], and the generation of informative pseudo-labels [9], [19], [20]. Due to limited regional text alignment capability of CLIP, some OVD models are directly trained on large-scale datasets for various tasks, such as object detection [21]–[23], image captioning [24], [25], and phrase grounding [22], [26] etc., to enrich semantic understanding and improve the detection ability of OVD models. However, despite the inclusion of a rich attribute vocabulary in training datasets, recent studies [10] have shown that mainstream OVD models perform poorly in detecting objects with fine-grained attributes. Under the mainstream evaluation protocol for only category names, OVD models suppress the fine-grained attributes that are explicitly composited in global text features [27].

Consequently, the development of specialized datasets and methods for fine-grained open vocabulary detection is crucial for advancing the precision and granularity of OVD models.

B. Fine-Grained Open Vocabulary Object Detection

Traditional fine-grained object detection focuses on inter-class differences [28]–[31], such as distinguishing between Samoyed and Labrador dogs, and lack the capability to detect objects outside their training categories. In contrast, FG-OVD is more concerned with intra-class extrinsic attributes, such as "brown dog" or "black dog", offering greater generality. However, research on FG-OVD models is currently scarce. Most works focus on fine-grained categorization, e.g., DetCLIPv3 [32] generates and trains on hierarchical category labels to enhance category-level fine-grained capabilities, while real-world objects are more complex with attribute-level granularity.

Differently, this paper is dedicated to exploring attribute-level fine-grained open vocabulary detection methods. The study reveals that existing OVD models all incorporate text encoders based on the Transformer architecture [33], mainly based on CLIP text encoder architecture [2], [3], [8], [9], [16], [18], [34], [35], and BERT architecture [4], [5], [7]. Our proposed method can enhance text attribute features through linear combination to activate attribute features that exist but are suppressed by mainstream OVD models.

C. Large Language Models as Auxiliary Tools

LLMs [14], [36], due to their emergent comprehension and generation abilities to generate answers following user instructions, are increasingly being utilized to assist in various natural language processing tasks. For instance, OVD model DetCLIPv3 [32] employs an LLM to annotate images with rich hierarchical object labels. Similarly, the FG-OVD dataset [10] comprises both positive and negative captions generated by an LLM. In this paper, the capabilities of LLM are leveraged to extract attributes in input text, thereby aiding OVD models in focusing on and enhancing attribute features. This approach is designed to improve the sensitivity of OVD models to fine-grained attributes and their overall performance on fine-grained open-vocabulary object detection.
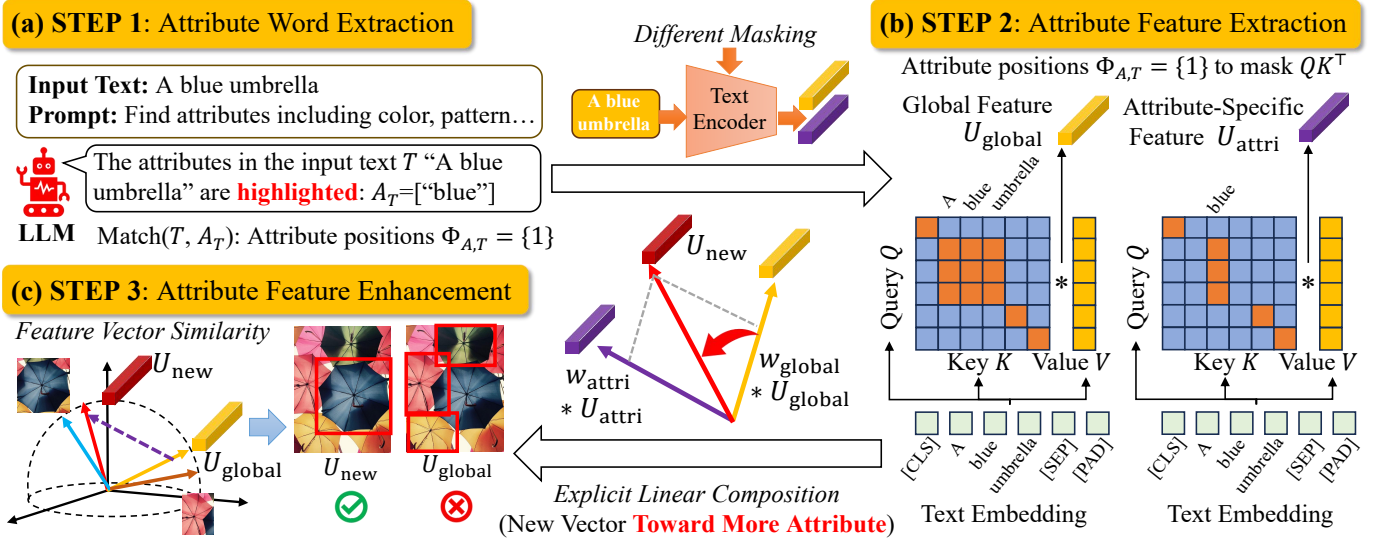
Fig. 2. The overall architecture of our proposed HA-FGOVD approach. (a) Firstly, a LLM follows the prompt to highlight the attributes in input text, which are then converted into attribute positions $\Phi_{A,T}$. (b) Secondly, $\Phi_{A,T}$ are employed to mask the attention map $QK^\top$ to obtain attribute specific feature U_{attri}. (c) Finally, explicit linear composition yields new feature U_{new} from U_{attri} and U_{global} toward more attribute, which enhances the final detection results.

III. PROPOSED METHOD

As illustrated in Fig. 2, we propose a universal approach to enhance the attribute-level OVD capabilities of mainstream models by highlighting fine-grained attributes in an explicit linear space. To amplify the fine-grained attribute features that exist but are suppressed in the frozen OVD models, our architecture consists of three key process: Attribute Words Extraction, Attribute Feature Extraction and Attribute Feature Enhancement.

A. Attribute Words Extraction

To assist the OVD models in focusing on attribute words, we employed the LLAMA2 [14] LLM to extract attribute words from the input text. As shown in Fig. 3, to ensure the precision and standardization of the output, we configure the LLM within the system message to establish a general dialogue background which sets the model as the role of extracting the attribute words, and provides the definition of the attribute word as well as the output format. In addition, several in-context examples are supplied to aid the model in understanding the output rules. The specific output format is defined to include only attribute words, separated by spaces, without any other vocabulary, in the form of [attribute1 attribute2 ... attributeN]. When no attribute word is detected in the statement, the output should be [None].

Given the prompt instruction P and input text T, the LLM predicts the set of N attribute words $A_T = \{a_i \in T\}$:

$$A_T = \text{LLM}(P, T) = \{a_i \in T \mid 0 \le i \le N\} \quad (1)$$

Then the position of each attribute word is obtained by matching function with the input text T:

$$\Phi_{A,T} = \text{Match}(\text{Tokenize}(T), \text{Tokenize}(A_T))$$
$$= \{\phi_i \in [0, L] \mid 0 \le i \le N\} \quad (2)$$
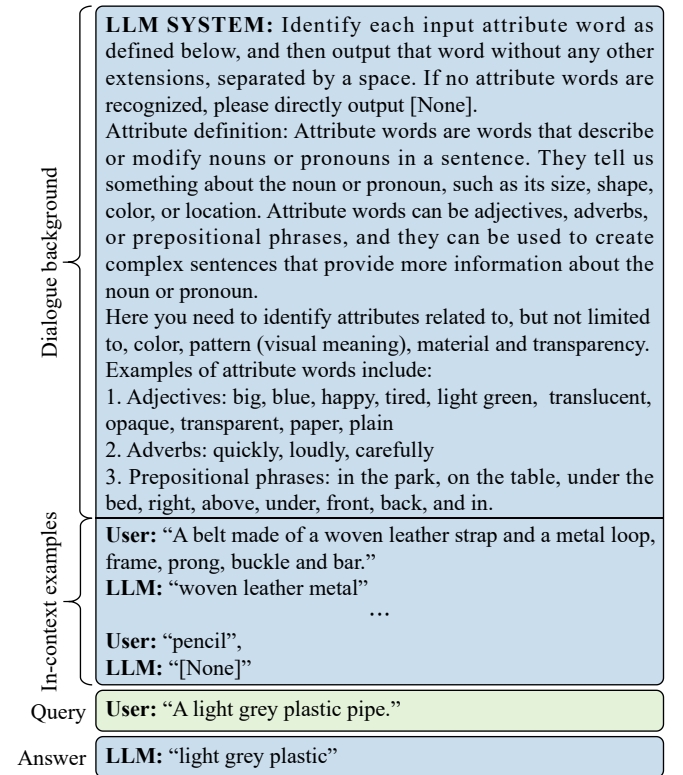
Fig. 3. Attribute Words Extraction. The LLM is configured within the system message to establish a general dialogue background. This configuration defines the model's role as extracting attribute words and provides the definition of attribute words as well as the output format. In addition, 15 in-context examples are given to aid the LLM in comprehending the output rules, with the aim of improving the precision of attribute words extraction and reducing the risk of hallucinations.

B. Attribute Feature Extraction

As mentioned in Section II, all models we have surveyed include a text encoder structure and are based on variations

(a) Default Mask for U_{global}   **(b) Attribute Mask for U_{attri}**

Fig. 4. 2D attention masks in text encoder of BERT architecture. (a) Default mask for global feature U_{global} and (b) attribute mask for attribute-specific feature U_{attri}. Take the 2nd token "[T$_2$]" as attribute for an example.
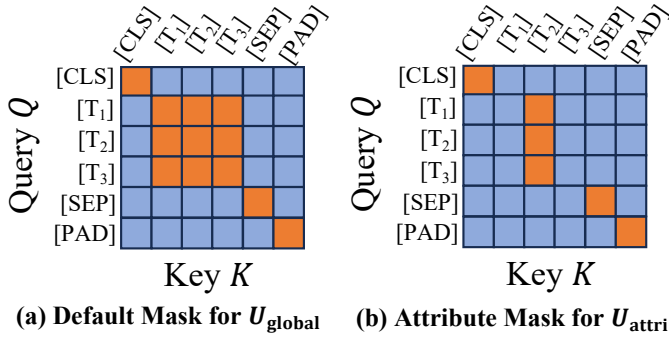

(a) Default Mask for U_{global}   **(b) Attribute Mask for U_{attri}**
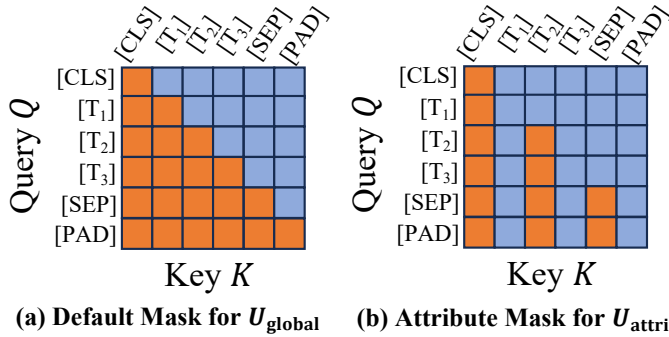
Fig. 5. 2D attention masks in text encoder of CLIP architecture. (a) Default mask for global feature U_{global} and (b) attribute mask for attribute-specific feature U_{attri} . Take the 2nd token "[T$_2$]" as attribute for an example.

of the Transformer architecture, specifically the CLIP [12] or BERT [37] models. These models utilize token attention masks to guide the text encoder in extracting text information from specified positions when encoding input text. Considering that the semantic information of attribute words depends on different contexts, for example, the contextual semantic information of "blue" in "a blue dog" and "a blue umbrella" is different, and in order to ensure consistency of the positional information between the global text features and attribute features, attribute features are not extracted from individual attribute words.

Instead, we have highlighted attribute semantic information by retaining the token attention masks of attribute and masking non-attribute tokens. Subsequently, we combine the global text features with attribute features through a linear weighting composition to form an attribute-highlighted text feature, which is then utilized for object detection.

The method is applied following the original models' token attention mask structures and making adaptive adjustments.

BERT architecture [37] employs a vanilla self-attention mechanism which allows each element in the sequence to interact with all other elements within the sequence. Due to the model's special handling of attention masks for special tokens, such as the initial [CLS], separator [SEP], and padding [PAD] tokens (as illustrated in Fig. 4), this algorithm operates only on the token attention masks between the [CLS] and [SEP] tokens.

Given an attention map $QK^\top \in \mathbb{R}^{(L+3) \times (L+3)}$, its default

2D attention mask $M \in \{-\infty, 0\}^{L \times L}$ is derived as:

$$\bar{M} = \Psi\Psi^\top + \text{diag}(1 - \Psi), \quad M = [(1 - \bar{M}) \odot -\infty], \quad (3)$$

which is further based on the 1D token mask as a vector $\Psi = [\Psi_0, \Psi_1, \cdots, \Psi_{L+1}, \Psi_{L+2}]^\top$ with elements $\Psi_i = 1$ as text tokens and $\Psi_i = 0$ as special tokens [CLS], [PAD] and [SEP]:

$$\Psi_i = \begin{cases} 0, & i = 0 \ , \ i > L \\ 1, & 1 \leq i \leq L \end{cases}. \quad (4)$$

Therefore, $\Psi\Psi^\top$ means that 2D attention is computed across the tokens of input text, while $\text{diag}(1 - \Psi)$ handles the special tokens at $\Psi_i = 0$ positions in $1 - \Psi$ as a Diagonal Matrix.

With the attention mask M, global feature U_{global} is obtained via the self-attention mechanism with query Q, key K and value V features of the text and special tokens as:

$$U_{\text{global}} = \text{softmax}\left(\frac{QK^\top}{\sqrt{d_K}} + M\right)V, \quad (5)$$

where each attention value added with $-\infty$ in attention mask M yields $e^{-\infty} = 0$ inside $\text{softmax}(\cdot)$ function for the lowest attention, and other value added with 0

To keep attribute-specific tokens, we employ the attribute position $\Phi_{A,T}$ from LLM as a new 1D token mask with elements Θ_i:

$$\Theta_i = \begin{cases} 0, & i \in \Phi_{A,T} \\ 1, & i \notin \Phi_{A,T} \end{cases} \quad (6)$$

Attribute-specific feature U_{attri} is obtained similar to U_{global} via new M^* to obtain M^*:

$$\bar{M}^* = \Theta\Psi^\top + \text{diag}(1 - \Psi) \quad (7)$$

The 3D attention mask processing pseudocode is presented as Algorithm 1. The bs and num_text_tokens are used for batch size and the number of text tokens. The value $True$ indicates that the token is not masked, and $False$ indicates that it is masked.

CLIP architecture [12] employs a lower triangular matrix causal attention mechanism, which is a special kind of self-attention mechanism. This mechanism introduces directionality into the sequence model, ensuring that when calculating the representation of the current element, only the positions before the current element are considered, without including those after it. As shown in Fig. 5, unlike self-attention, causal attention does not perform special processing on the attention mask corresponding to the special token. Since [CLS] tokens and [SEP] tokens contain global and location information [38], [39], these two special tokens are not masked when extracting attribute features. The [PAD] token is masked which has no practical meaning.

Default 2D attention mask $M \in \{-\infty, 0\}^{L \times L}$ is derived as a Lower Triangle Matrix:

$$M_{i,j} = \begin{cases} 0, & i \geq j \\ -\infty, & i < j \end{cases} \quad (8)$$

Now given the attribute position $\Phi_{A,T}$ from LLM, we have new 2D mask M^*:

$$M_{i,j}^* = \begin{cases} 0, & i \geq j \ and \ j \in \Phi_{A,T} \\ -\infty, & otherwise \end{cases} \quad (9)$$

Algorithm 1 HF-FGOVD Algorithm Pipeline

FUNC MATCH($Token_{\mathbf{cap}}, Token_{\mathbf{attri}}$)
　$Position_{\mathbf{attri}}[bs, num\_text\_tokens] \leftarrow False$
　for $bs, (cap, attri)$ **in** $enum(Token_{\mathbf{cap}}, Token_{\mathbf{attri}})$:
　　$index \leftarrow [i \ \mathbf{if} \ cap_i = attri_j]$
　　if $model$ **is** $"BERT"$:
　　　$index \leftarrow index + [i \ \mathbf{if} \ cap_i = [\text{PAD}]]$
　　$Position_{\mathbf{attri}}[bs][index] \leftarrow True$
　return $Position_{\mathbf{attri}}$

FUNC TEXT_ENCODER($Caption, Attribute, \theta'$)
　$w_{\mathbf{global}}, w_{\mathbf{attri}}, \text{bias} \leftarrow \theta'$
　$Token_{\mathbf{cap}} \leftarrow \text{Tokenize}(Caption)$
　$Mask_{\mathbf{cap}} \leftarrow \text{Generate\_Mask}(Token_{\mathbf{cap}})$
　$Feature_{\mathbf{cap}} \leftarrow \text{Attention}(Token_{\mathbf{cap}}, Mask_{\mathbf{cap}})$
　if $Attribute$ **is not** $None$:
　　$Token_{\mathbf{attri}} \leftarrow \text{Tokenize}(Attribute)$
　　$Position_{\mathbf{attri}} \leftarrow \text{Match}(Token_{\mathbf{cap}}, Token_{\mathbf{attri}})$
　　$Mask_{\mathbf{attri}} \leftarrow \text{Eq. 7 or Eq. 9}$
　　$Feature_{\mathbf{attri}} \leftarrow \text{Attention}(Token_{\mathbf{cap}}, Mask_{\mathbf{attri}})$
　　$Feature_{\mathbf{cap}} \leftarrow w_{\mathbf{global}} \times Feature_{\mathbf{cap}}+$
　　　　　　　　$w_{\mathbf{attri}} \times Feature_{\mathbf{attri}} + \text{bias}$
　return $Feature_{\mathbf{cap}}$

FUNC TRAIN($Images, Captions, Prompt, GTs$)
　$\theta' \leftarrow w_{\mathbf{global}}, w_{\mathbf{attri}}, \text{bias}$
　for $Image, Caption, GT$ **in** $Images, Captions, GTs$:
　　$Attribute \leftarrow \text{LLM}(Prompt, Caption)$
　　$Feature_{\mathbf{cap}} \leftarrow \text{Text\_Encoder}(Caption, Attribute, \theta')$

　　$Feature_{\mathbf{vis}} \leftarrow \text{Visual\_Encoder}(Image)$
　　$Pred \leftarrow \text{Detection}(Feature_{\mathbf{cap}}, Feature_{\mathbf{vis}})$
　　$\mathcal{L}_{\mathbf{det}} \leftarrow \mathcal{L}_{\mathbf{cls}}(Pred_{\mathbf{cls}}, GT_{\mathbf{cls}}) + \mathcal{L}_{\mathbf{reg}}(Pred_{\mathbf{reg}}, GT_{\mathbf{reg}})$
　　$\theta' \leftarrow \theta' - \eta\nabla_{\theta'}\mathcal{L}_{\mathbf{det}}$
　return $w_{\mathbf{global}}, w_{\mathbf{attri}}, \text{bias}$

Both global feature U_{global} and attribute-specific feature U_{attri} are obtained similar to self-attention equation in BERT. The algorithm can also be represented by Algorithm 1.

C. Attribute Feature Enhancement

In the field of multimodality, embeddings of composite concepts can often be well-approximated as linear compositional structures [13], such as $U(\text{rainy morning}) = U(\text{rainy}) + U(\text{morning})$. Leveraging the linear additivity of embeddings, we perform a weighted linear fusion of global text features and attribute features as two vectors, which can be mathematically represented as follows:

$$U_{\text{global}} = U_{\text{attri}} + U_{\text{cate}},$$
$$U_{\text{new}} = w_{\text{global}}U_{\text{global}} + w_{\text{attri}}U_{\text{attri}}$$
$$\Rightarrow U_{\text{new}} = w_{\text{global}}\left(U_{\text{attri}} + U_{\text{cate}}\right) + w_{\text{attri}}U_{\text{attri}}$$
$$\Rightarrow U_{\text{new}} = \left(w_{\text{global}} + w_{\text{attri}}\right)U_{\text{attri}} + w_{\text{global}}U_{\text{cate}} \quad (10)$$

where U_{global} and U_{attri} are the vectors for global text and the attribute words, respectively, while w_{global} and w_{attri} denote

their corresponding weight scalars. According to the reasoning formula, the new features U_{new} are enhanced more towards U_{attri}, with $w_{\text{global}} + w_{\text{attri}}$ higher than w_{global} for category features U_{cate}. Moreover, an extra bias can be further applied to U_{new} for a better learning of explicit linear composition:

$$U_{\text{new}} = w_{\text{global}}U_{\text{global}} + w_{\text{attri}}U_{\text{attri}} + \text{bias}. \quad (11)$$

The U_{new} signifies the attribute-highlighted embedding. U_{new} is the output of the text encoder for detection tasks. The scaler weight triplets are represented as $(w_{\text{global}}, w_{\text{attri}}, \text{bias})$.

IV. EXPERIMENTS

We report the performance of applying our method to three models of different architectures, which are fine-tuned in the FG-OVD [10] training set and tested on this benchmark. In "Experimental Settings" Section, FG-OVD dataset and evaluation protocol is introduced. The three models are introduced in "Baseline Methods" Section. Then, we present the fine-tuning schemes and compare the fine-tuned FG-OVD performance with the baselines and previous works.

Since only three parameter scalars for the explicit linear composition are fine-tuned, they have strong transferability. Hence, we report the test performance after transferring the best weight scalars triplets of the three models to each other.

A. Experimental Settings

FG-OVD benchmark: The FG-OVD dataset [10] is a comprehensive dataset with eight distinct scenarios, divided into difficulty-based and attribute-based benchmarks. Each subset consists of both positive and negative captions, which are essential for a balanced assessment. The difficulty-based benchmarks adjust the negative captions to make the lower or higher distinction between positive and negative captions, with the Trivial, Easy, Medium, and Hard subsets representing increasing levels of challenge. In details, negative captions of Trivial are arbitrarily selected from other objects, while Easy, Medium, and Hard are crafted by successively replacing 3, 2, and 1 attributes, in that order. On the other hand, the attribute-based benchmarks enable a more focused evaluation of OVD models to detect objects with a specific kind of attributes types, including Color, Material, Pattern and Transparency.

Evaluation Protocol: The Evaluation Protocol for this paper strictly adheres to the settings of FG-OVD dataset [10], employing dynamic vocabularies for both training and inference. This means that for each detected object i, the model identifies a category from $\{c_i^{\text{pos}}, c_{i,1}^{\text{neg}}, ..., c_{i,N}^{\text{neg}}\}$, Here, c_i^{pos} signifies the positive description of the object i, while $c_{i,1}^{\text{neg}}$ represents the first negative caption for object i, with a total of N. As depicted in the formula [40], traditional evaluation metrics do not penalize the presence of an incorrect prediction with higher confidence occurring at the correct location.

For instance, assuming a OVD model is tasked with detecting a category with a positive caption "red house" and a negative caption "green house", if the model fails to comprehend the semantic context of the text, it may detect two bounding boxes at the location of the ground truth "red house" and assign both these two labels accordingly.

TABLE I
DIFFERENCES AMONG DETIC, GROUDING DINO, AND OWL-VIT MODELS, INCLUDING THEIR OVERALL ARCHITECTURE AND TEXT ENCODERS. TEXT EMBEDDING FLOW MEANS HOW TEXTUAL FEATURES FROM TEXT ENCODER ARE UTILIZED FOR OVD. VIEMBED MEANS VISUAL EMBEDDING.

Model	Overall Architecture	Text Encoder Type	Text Encoder Attention Type	Text Embedding Flow
Detic	Two-stage	CLIP (pretrained)	Causal-Attention	Replace the classifier weights
Grounding DINO	End-to-end	BERT (pretrained)	Self-Attention	Calculate similarity after cross-fused with the ViEmbed
OWL-ViT	End-to-end	CLIP (fine-tuned)	Causal-Attention	Calculate similarity with ViEmbed

In this way, the OVD model could trick the evaluation metrics, achieving an accuracy of 0.5 and a recall of 1.0 for that category. And if this scenario is consistent across all categories tested, the final mean average precision (mAP) would also be 0.5:

$$Precision = \frac{TP}{TP+FP} = \frac{1}{1+1} = 0.5, \quad (12)$$

$$Recall = \frac{TP}{\text{num}(GT)} = \frac{TP}{TP+FN} = \frac{1}{1+0} = 1, \quad (13)$$

where TP denotes the count of instances correctly identified for a particular category, whereas FP and FN refer to the instances that are mistakenly classified as part of that category or exist in ground truth GT but not detected. $\text{num}(GT)$ signifies the overall number of ground-truth instances present in the image. To accurately assess the model's fine-grained open-vocabulary detection capabilities, a class-agnostic NMS [10] is applied in post-processing ensure that only one prediction per location is retained, irrespective of the class label.

When testing on the benchmark, we follow the configuration from [10], selecting 5 negative captions (N=5) in the difficulty-based sub-datasets and 2 (N=2) in the attribute-based sub-datasets for each category.

B. Baseline Methods

As shown in Table I, the method proposed in this paper is applied to three distinct architecture-based OVD models: Detic [3], Grounding DINO [4] and OWL-ViT [2].

Detic [3] is trained jointly with image classification and object detection datasets to respectively expand detector vocabulary and enhance the classification and regression ability of the model. A mainstream two-stage object detection framework [41], [42] is employed with the classification weights W replaced by CLIP embeddings of class names to transform a conventional detector into an open-vocabulary detector.

Grounding DINO [4], a Referring Expression Comprehension (REC) model, is capable of detecting any object as per the user's input of categories or indicative expressions. It enhances the closed-set Transformer-based detector, DINO, by incorporating multi-phase vision-language modality fusion. Furthermore, the text encoder component of Grounding DINO [4] is based on a pre-trained BERT model.

OWL-ViT [2] is an end-to-end vision Transformer (ViT) architecture that replaces the fixed classification layer weights with class-name embeddings derived from a text model. This text model is fine-tuned based on the CLIP [12] text encoder.

OWL [2] and Detic [3] both utilize a text encoder based on the CLIP [12] architecture, and their token attention mask structures are similar. Specific numerical values are used to represent the degree of encoding importance, typically using an extremely small value $-\infty$ to denote no encoding and 0 for encoding, while they are marked by False and True in OWL model and then further converted into $-\infty$ and 0, correspondingly.

Model Architectural Settings: Implementation details of the baseline OVD models evaluated in this paper adhere to these settings following the paper of FG-OVD dataset [10]:

- OWL-ViT: ViT L/14 backbone version.
- Detic: `Detic_LCOCOI21k_CLIP_SwinB_896b32_4x_ft4x_max-size`, i.e., Swin-B backbone version with ImageNet-21K pre-training.
- Grounding Dino: Swin-T backbone version, i.e., the GroundingDINO-T configuration.

C. Fine-Tuning Schemes

As depicted in the Table II, upon statistical analysis of the trainable data within each subsets of the FG-OVD training set, all 8 subsets contain 27,684 category annotations. However, a significant portion of the positive captions lacks corresponding negative captions (N=0), which does not meet the training requirements set for this task. To ensure the balance of the training data, we selected 1,000 complete samples from each sub-datasets which include both positive and negative captions to form a new training set. Accordingly, 100 samples from each subsets in validation set to create a new validation set, while testing set is not changed for a fair comparison.

In this paper, for training the Detic [3] and OWL-ViT [2] models, we utilize the corresponding loss functions from their original papers, which are the standard losses in a two-stage detector and a bipartite matching loss similar to that introduced by DETR respectively. However, since Grounding DINO [4] is primarily a REC model, it differs from other detectors in that it cannot accept a vocabulary of captions as input. Therefore, following the inference approach in [10], we perform individual forward passes for each caption in the vocabulary and then calculate a bipartite matching loss for the predictions corresponding to the positive captions, similar to the loss used in OWL-ViT [2]. Only the classification loss is computed for the negative captions without ground truth bounding boxes. For classification loss for both positive and negative captions, we adhere to the original Grounding DINO [4] training method, setting the target binary classification label to 1 for each positive caption token and to 0 for the negative captions.

D. State-of-the-Art Comparison on FG-OVD Dataset

Table III shows the accuracy on the benchmark dataset before and after applying the HA-FGOVD method proposed

TABLE II
FG-OVD STATISTICS FOR TRAINING AND VALIDATION SETS.
WITH NEG. CAPTION INDICATES THAT THE CATEGORY CONTAINS NEGATIVE CAPTIONS.

Datasets	Hard	Medium	Easy	Trivial	Color	Material	Pattern	Transp.
training set	27684	27684	27684	27684	27684	27684	27684	27684
with negative caption	27683	24513	14178	27683	25215	25751	6020	2326
validation set	1444	1270	761	1444	1326	1321	322	119
with negative caption	1444	1270	761	1444	1326	1321	322	119

TABLE III
MAP EVALUATION RESULTS ON BENCHMARK (%). AVERAGE IS AVERAGED OVER THE 8 SUB-DATASETS. MAP FROM OWL-VIT(B/16) TO CORA
COMES FROM PREVIOUS WORK [10]. OTHER MAP RESULTS ARE BASED ON THE EXPERIMENTS AND REPRODUCTION (*) FROM OUR RESEARCHES.

Detector	Hard	Medium	Easy	Trivial	Color	Material	Pattern	Transp.	Average
OWL-ViT(B/16)	26.2	39.8	38.4	53.9	45.3	37.3	26.6	**34.1**	37.7
OWL-ViT(L/14)	26.5	39.3	44.0	65.1	43.8	44.9	36.0	29.2	41.1
OWLv2(B/16)	25.3	38.5	40.0	52.9	45.1	33.5	19.2	28.5	35.4
OWLv2(L/14)	25.4	41.2	42.8	63.2	**53.3**	36.9	23.3	12.2	37.3
Detic	11.5	18.6	18.6	69.7	21.5	38.8	30.1	24.6[1]	29.3
ViLD	22.1	36.1	39.9	56.6	43.2	34.9	24.5	30.1	35.9
Grounding DINO	16.6	27.9	30.1	62.7	41.0	30.2	31.2	25.4	33.1
CORA	13.8	20.0	20.4	35.1	25.0	19.3	22.0	27.9	22.9
Detic*	11.5	18.6	18.8	69.7	21.6	38.8	30.3	24.8	29.3
+ HA-FGOVD	12.2 (+0.7)	22.0 (+3.4)	19.8 (+1.0)	**70.3** (+0.6)	23.7 (+2.1)	41.0 (+2.2)	32.1 (+1.8)	25.5 (+0.7)	30.8 (+1.5)
Grounding DINO*	17.0	28.4	31.0	62.5	41.4	30.3	31.0	26.2	33.5
+ HA-FGOVD	19.2 (+2.2)	32.3 (+3.9)	34.0 (+3.0)	62.2 (-0.3)	41.5 (+0.1)	33.0 (+2.7)	32.1 (+1.1)	29.2 (+3.0)	35.4 (+1.9)
OWL-ViT(L/14)*	26.6	39.8	44.5	67.0	44.0	45.0	36.2	29.2	41.5
+ HA-FGOVD	**31.4** (+4.8)	**46.0** (+6.2)	**50.7** (+6.2)	67.2 (+0.2)	48.4 (+4.4)	**48.5** (+3.5)	**38.0** (+1.8)	32.7 (+3.5)	**45.4** (+3.9)

TABLE IV
TRANSFER RESULT OF WEIGHT SCALAR TRIPLETS (%). AVERAGE IS AVERAGED OVER THE 8 SUB-DATASETS. THE **BOLDEN** REPRESENTS THE HIGHEST
MAP ON THE SAME MODEL ARCHITECTURE. ($\leftarrow Training$) MEAN THE WEIGHT SCALAR TRIPLETS IS FROM TRAINING. ($\leftarrow Model$) MEANS TO APPLY
THE BEST WEIGHT SCALAR TRIPLETS OF THE MODEL TO THE BASELINE. THE BEST WEIGHT SCALAR TRIPLETS $(w_{global}, w_{attri}, bias)$ FOR EACH
MODEL IS: DETIC(0.434, 0.244, 0.250), GROUNDING DINO(0.565, 0.264, -0.178), OWL-VIT(0.772, 0.248, -0.080). THE BIAS IS SET TO 0 WHEN
TRANSFERRING TO ANOTHER MODEL.

Detector	Hard	Medium	Easy	Trivial	Color	Material	Pattern	Transp.	Average
Detic	11.5	18.6	18.8	69.7	21.6	38.8	30.3	24.8	29.3
$\leftarrow$ Training	**12.2** (+0.7)	**22.0** (+3.4)	**19.8** (+1.0)	**70.3** (+0.6)	**23.7** (+2.1)	**41.0** (+2.2)	**32.1** (+1.8)	25.5 (+0.7)	**30.8** (+1.5)
$\leftarrow$ Grounding DINO	12.0 (+0.5)	21.4 (+2.8)	18.6 (-0.2)	68.2 (-1.5)	21.8 (+0.2)	39.5 (+0.7)	31.6 (+1.3)	26.4 (+1.6)	29.9 (+0.6)
$\leftarrow$ OWL-ViT(L/14)	11.9 (+0.4)	21.0 (+2.4)	18.8 (+0.0)	69.8 (+0.1)	22.5 (+0.9)	40.5 (+1.7)	31.9 (+1.6)	**26.6** (+1.8)	30.4 (+1.1)
Grounding DINO	17.0	28.4	31.0	62.5	41.4	30.3	31.0	26.2	33.5
$\leftarrow$ Training	**19.2** (+2.2)	**32.3** (+3.9)	**34.0** (+3.0)	62.2 (-0.3)	**41.5** (+0.1)	**33.0** (+2.7)	**32.1** (+1.1)	29.2 (+3.0)	**35.4** (+1.9)
$\leftarrow$ Detic	18.3 (+1.3)	30.2 (+1.8)	32.6 (+1.6)	**62.9** (+0.4)	41.3 (-0.1)	31.5 (+1.2)	30.4 (-0.6)	27.7 (+1.5)	34.4 (+0.9)
$\leftarrow$ OWL-ViT(L/14)	19.0 (+2.0)	31.1 (+2.7)	33.5 (+2.5)	62.7 (+0.2)	41.3 (-0.1)	32.1 (+1.8)	31.7 (+0.7)	**30.0** (+3.8)	35.2 (+1.7)
OWL-ViT(L/14)	26.6	39.8	44.5	67.0	44.0	45.0	36.2	29.2	41.5
$\leftarrow$ Training	31.4 (+4.8)	46.0 (+6.2)	50.7 (+6.2)	**67.2** (+0.2)	48.4 (+4.4)	48.5 (+3.5)	38.0 (+1.8)	**32.7** (+3.5)	**45.4** (+3.9)
$\leftarrow$ Detic	30.2 (+3.6)	44.1 (+4.3)	47.2 (+2.7)	**67.2** (+0.2)	47.7 (+3.7)	46.8 (+1.8)	**38.3** (+2.1)	30.6 (+1.4)	44.0 (+2.5)
$\leftarrow$ Grounding DINO	**32.4** (+5.8)	**48.1** (+8.3)	**51.5** (+7.0)	66.9 (-0.1)	**49.0** (+5.0)	**48.9** (+3.9)	35.8 (-0.4)	29.3 (+0.1)	45.2 (+3.7)

in this paper, and comparing with previous state-of-the-art methods. Our proposed HA-FGOVD approach achieves an overall increase in accuracy when applied to each model. The Trivial subset exhibits minor fluctuations due to the fact that the positive and negative captions are completely dissimilar texts with inherently significant differences in their textual features. Consequently, the effect of enhancing attribute features to differentiate these textual differences is minimal. In individual sub-datasets, the proposed approach can achieve the highest accuracy improvement of up to 6.2%.

---

[1] The authors corrected the value to 24.6 instead of 28, as indicated on the GitHub homepage of the paper [10]. For further details, please refer to the official code repository: https://github.com/lorebianchi98/FG-OVD.

Significantly, these experimental results show that the original text features of the OVD model indeed contain attribute features which are suppressed. By highlighting and enhancing attribute features and linearly combining them with global text features, attribute information can be activated, thus improving the detection ability of FG-OVD. After applying this method, the performance on multiple sub-datasets of the OWL-ViT model, as well as the average value of all subsets, reaches the state-of-the-art (SOTA) performance on the FG-OVD dataset.

E. Transfer Evaluation of Explicit Weight Scalar Triplets

To assess the transferability of the explicit weight scalar triplets among various OVD models, we transfer the optimal

TABLE V
OVERALL ABLATION STUDY ON OWL-VIT(L/14) BASELINE FOR KEY FACTORS OF OUR PROPOSED HA-FGOVD, INCLUDING WITHOUT BIAS, MASK THE FIRST AND LAST TOKENS ([CLS] AND [SEP]) AND AND MASK RANDOM WORDS BASED ON THE PROPOSED METHOD, RESPECTIVELY. **BOLDEN** ARE THE BEST RESULTS.

Methods	Hard	Medium	Easy	Trivial	Color	Material	Pattern	Transp.	Average
baseline	26.6	39.8	44.5	67.0	44.0	45.0	36.2	29.2	41.5
w/o bias	**31.6** (+5.0)	**46.0** (+6.2)	**50.9** (+6.4)	67.0 (+0.0)	**48.6** (+4.6)	48.3 (+3.3)	36.9 (+0.7)	30.3 (+1.1)	45.0 (+3.5)
mask [CLS] **&** [SEP]	29.0 (+2.4)	43.0 (+3.2)	45.3 (+0.8)	67.1 (+0.1)	46.6 (+2.6)	47.3 (+2.3)	35.1 (-1.1)	31.6 (+2.4)	43.1 (+1.6)
mask random words	23.7 (-2.9)	38.6 (-1.2)	42.5 (-2.0)	66.8 (-0.2)	40.9 (-3.1)	42.9 (-2.1)	31.1 (-5.1)	25.7 (-3.5)	39.0 (-2.5)
HA-FGOVD (ours)	31.4 (+4.8)	**46.0** (+6.2)	50.7 (+6.2)	**67.2** (+0.2)	48.4 (+4.4)	**48.5** (+3.5)	**38.0** (+1.8)	**32.7** (+3.5)	**45.4** (+3.9)

A black wooden chair.
A dark purple wooden chair.
A yellow wooden chair.
A black paper chair.
A black plastic chair.
A red text bowl.

A white ceramic bowl.
A yellow leather bowl.
A dark brown fabric bowl.
A purple metal bowl.
A blue text bowl.
A black metal chair.

A red striped leather back of a bench.
A dark yellow striped crochet back of a bench.
A blue perforated leather back of a bench.
A red floral plastic back of a bench.
A dark brown checkered leather back of a bench.
A dark blue dotted leather back of a bench.

A woven light brown wood basket.
A perforated light brown wood basket.
A striped light brown wood basket.

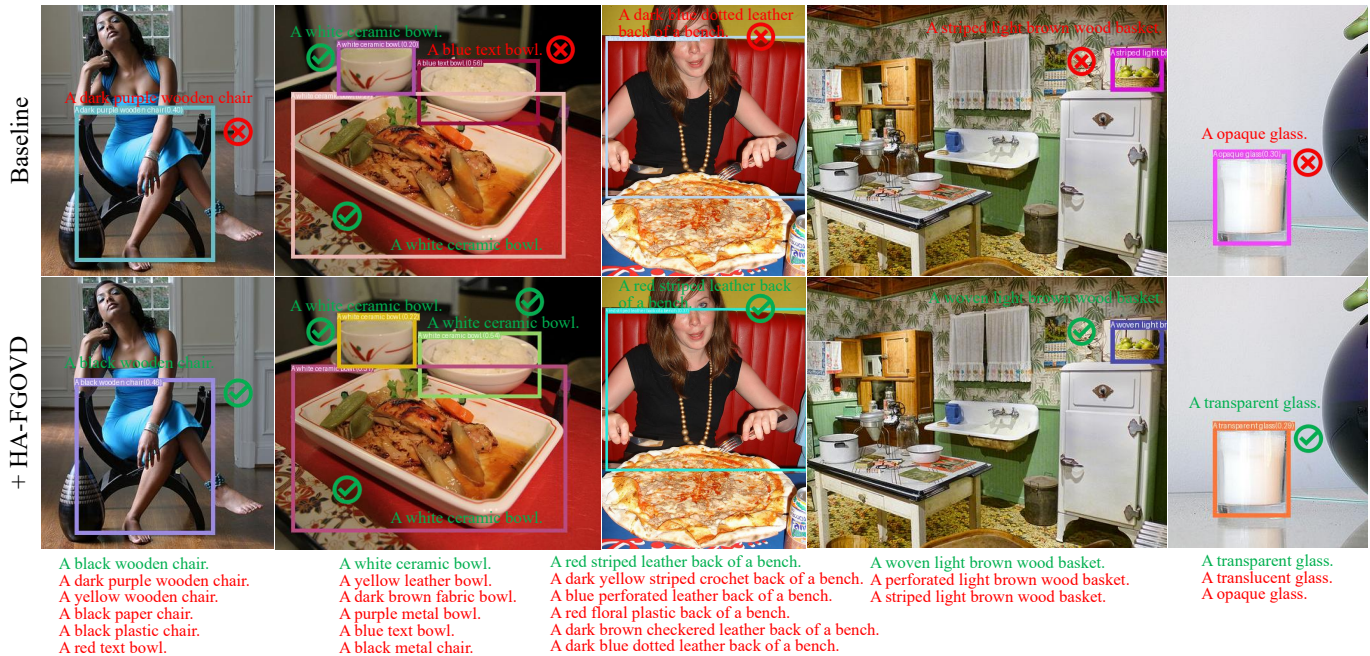A transparent glass.
A translucent glass.
A opaque glass.

Fig. 6. The visualization of the detection results before and after applying our proposed HA-FGOVD approach on OWL-ViT baseline. At the bottom are the captions utilized for detection during the inference phase, with positive captions highlighted in green and negative captions in red. The initial row corresponds to the baseline results, which exhibit inaccuracies. The subsequent row delineates the refined results after applying our proposed HA-FGOVD approach, effectively corrects the aforementioned errors.

triplets from one model to another, and then evaluate their performance, as demonstrated in the Table IV.

In the theory of deep learning, the bias parameter typically aiding in better data fitting of the models. Compared to the feature representation layers that capture universal features, such as the weights of convolutional layers, the value of bias is usually more specific to the particular model and task [43]. Therefore, when testing the transfer performance of weight scalar triples, we set the bias to 0 for all.

Under the transferred parameter settings, the overall accuracy of the models can still increase. But the overall accuracy of the triplets obtained through training is more superior. Furthermore, the accuracy of several datasets surpasses that of the trained parameters. This indicates that when the training set is balanced, the parameters obtained by training are globally optimal. Otherwise, the models may reach a local optimum.

F. Ablation Study

We investigate the key factors for our method to work in Table V. The ablation study is conducted with the best-performed OWL-ViT model under the same experiment settings.

The 1st row in Table V presents the mAP of the OWL-ViT baseline, while the last row illustrates the accuracy of our method. The 2nd row delineates the results without the bias parameter in Eq. 11. Although non-bias setting still yields performance gain from the baseline, incorporation of the bias parameter leads to higher overall accuracy. This suggests that the bias can better fit all types of data by linearly translating attribute features, thereby achieving a global optimum.

To explore the significance of the initial and separator special tokens ([CLS], [SEP]) in extracted attribute features, the results of masking these tokens are reported in the 3rd row. The data indicate that most sub-datasets exhibit an increase in performance; however, the accuracy of the pattern subset declines by 1.1% compared to the baseline. In contrast, our proposed method, which does not mask the two tokens, demonstrates substantial improvements across all sub-datasets. This indicates that the special tokens in text encoders encompass vital fine-grained information that should not be masked.

Finally, to evaluate the LLM capability of highlighting attribute words, we conducted experiments by the random masking of certain input textual vocabularies, rather than at-

tribute positions from LLM. Specifically, during both training and testing, we randomly selected $[0, L-1]$ vocabularies to mask within an input of L words, effectively augmenting $[1, L]$ words. In the 4th row, mAP for all subsets decrease, indicating that attribute word extraction of LLM guarantees an improvement in fine-grained capabilities, thereby validating the effectiveness of our proposed approach.

G. Visualization

Fig. 6 provides the visualization results of OV detection for the baseline before and after applying the HA-FGOVD method. Our approach demonstrates excellent performance in improving the FG-OVD capability of mainstream OVD models, especially the complex input captions with a composition of various attribute types in 3rd and 4th columns in Fig. 6, as well as captions that hard to distinguished from each other in 1st, 2nd and 5th columns. In conclusion, our HA-FGOVD approach is robust and powerful enough to handle these challenging scenarios in FG-OVD task.

V. CONCLUSION

In this paper, we propose a universal FG-OVD approach, called HA-FGOVD, which is a plug-and-play manner for mainstream frozen OVDs to enhance their fine-grained object detection capabilities by making use of a simple but explicit linear composition. Extensive experiments have demonstrated that our approach can effectively activate the suppressed attribute features, proving that there is potential for attribute features within the latent space of mainstream OVD models. Moreover, the weight scalar triplets in our approach can be transferred to other OVD models without additional training. The proposed approach achieves new state-of-the-art performance on the FG-OVD benchmark.

REFERENCES

[1] J. Wu, X. Li, S. Xu, H. Yuan, H. Ding, Y. Yang, X. Li, J. Zhang, Y. Tong, X. Jiang, B. Ghanem, and D. Tao, "Towards open vocabulary learning: A survey," *IEEE Trans Pattern Anal Mach Intell*, vol. 46, no. 7, pp. 5092–5113, 2024. [Online]. Available: https://www.ncbi.nlm.nih.gov/pubmed/38315601

[2] M. Minderer, A. Gritsenko, A. Stone, M. Neumann, D. Weissenborn, A. Dosovitskiy, A. Mahendran, A. Arnab, M. Dehghani, and Z. Shen, "Simple open-vocabulary object detection," in *European Conference on Computer Vision*. Springer, Conference Proceedings, pp. 728–755.

[3] X. Zhou, R. Girdhar, A. Joulin, P. Krähenbühl, and I. Misra, "Detecting twenty-thousand classes using image-level supervision," in *European Conference on Computer Vision*. Springer, Conference Proceedings, pp. 350–368.

[4] S. Liu, Z. Zeng, T. Ren, F. Li, H. Zhang, J. Yang, C.-y. Li, J. Yang, H. Su, J.-J. Zhu, and L. Zhang, "Grounding dino: Marrying dino with grounded pre-training for open-set object detection," *ArXiv*, vol. abs/2303.05499, 2023.

[5] H. Zhang, P. Zhang, X. Hu, Y.-C. Chen, L. Li, X. Dai, L. Wang, L. Yuan, J.-N. Hwang, and J. Gao, "Glipv2: Unifying localization and vision-language understanding," *Advances in Neural Information Processing Systems*, vol. 35, pp. 36067–36080, 2022.

[6] J. Wu, X. Li, H. Yuan, H. Ding, Y. Yang, X. Li, J. Zhang, Y. Tong, X. Jiang, B. Ghanem, and D. Tao, "Towards open vocabulary learning: A survey," *ArXiv*, vol. abs/2306.15880, 2023.

[7] L. H. Li, P. Zhang, H. Zhang, J. Yang, C. Li, Y. Zhong, L. Wang, L. Yuan, L. Zhang, and J.-N. Hwang, "Grounded language-image pre-training," in *Proceedings of the IEEE/CVF Conference on Computer Vision and Pattern Recognition*, Conference Proceedings, pp. 10965–10975.

[8] L. Yao, J. Han, X. Liang, D. Xu, W. Zhang, Z. Li, and H. Xu, "Detclipv2: Scalable open-vocabulary object detection pre-training via word-region alignment," in *Proceedings of the IEEE/CVF Conference on Computer Vision and Pattern Recognition*, Conference Proceedings, pp. 23497–23506.

[9] Y. W. Zhong, J. W. Yang, P. C. Zhang, C. Y. Li, N. Codella, L. H. Li, L. W. Zhou, X. Y. Dai, L. Yuan, Y. Li, and J. F. Gao, "Regionclip: Region-based language-image pretraining," *2022 Ieee/Cvf Conference on Computer Vision and Pattern Recognition (Cvpr 2022)*, pp. 16772–16782, 2022. [Online]. Available: ⟨GotoISI⟩://WOS:000870783002057https://ieeexplore.ieee.org/stampPDF/getPDF.jsp?tp=&arnumber=9878561&ref=

[10] L. Bianchi, F. Carrara, N. Messina, C. Gennaro, and F. Falchi, "The devil is in the fine-grained details: Evaluating open-vocabulary object detectors for fine-grained understanding," in *Proceedings of the IEEE/CVF Conference on Computer Vision and Pattern Recognition*, Conference Proceedings, pp. 22520–22529.

[11] K. Chen, X. Jiang, Y. Hu, X. Tang, Y. Gao, J. Chen, and W. Xie, "Ovarnet: Towards open-vocabulary object attribute recognition," in *Proceedings of the IEEE/CVF conference on computer vision and pattern recognition*, Conference Proceedings, pp. 23518–23527.

[12] A. Radford, J. W. Kim, C. Hallacy, A. Ramesh, G. Goh, S. Agarwal, G. Sastry, A. Askell, P. Mishkin, and J. Clark, "Learning transferable visual models from natural language supervision," in *International conference on machine learning*. PMLR, Conference Proceedings, pp. 8748–8763.

[13] M. Trager, P. Perera, L. Zancato, A. Achille, P. Bhatia, and S. Soatto, "Linear spaces of meanings: compositional structures in vision-language models," in *Proceedings of the IEEE/CVF International Conference on Computer Vision*, Conference Proceedings, pp. 15395–15404.

[14] H. Touvron, L. Martin, K. Stone, P. Albert, A. Almahairi, Y. Babaei, N. Bashlykov, S. Batra, P. Bhargava, and S. Bhosale, "Llama 2: Open foundation and fine-tuned chat models," *arXiv preprint arXiv:2307.09288*, 2023.

[15] K. Zhou, J. Yang, C. C. Loy, and Z. Liu, "Learning to prompt for vision-language models," *International Journal of Computer Vision*, vol. 130, no. 9, pp. 2337–2348, 2022.

[16] X. Gu, T.-Y. Lin, W. Kuo, and Y. Cui, "Open-vocabulary object detection via vision and language knowledge distillation," *arXiv preprint arXiv:2104.13921*, 2021.

[17] Z. Ma, G. Luo, J. Gao, L. Li, Y. Chen, S. Wang, C. Zhang, and W. Hu, "Open-vocabulary one-stage detection with hierarchical visual-language knowledge distillation," in *Proceedings of the IEEE/CVF Conference on Computer Vision and Pattern Recognition*, Conference Proceedings, pp. 14074–14083.

[18] X. Wu, F. Zhu, R. Zhao, and H. Li, "Cora: Adapting clip for open-vocabulary detection with region prompting and anchor pre-matching," in *Proceedings of the IEEE/CVF Conference on Computer Vision and Pattern Recognition*, Conference Proceedings, pp. 7031–7040.

[19] L. Yao, J. Han, Y. Wen, X. Liang, D. Xu, W. Zhang, Z. Li, C. Xu, and H. Xu, "Detclip: Dictionary-enriched visual-concept paralleled pre-training for open-world detection," *Advances in Neural Information Processing Systems*, vol. 35, pp. 9125–9138, 2022.

[20] A. Zareian, K. D. Rosa, D. H. Hu, and S.-F. Chang, "Open-vocabulary object detection using captions," in *Proceedings of the IEEE/CVF Conference on Computer Vision and Pattern Recognition*, Conference Proceedings, pp. 14393–14402.

[21] A. Gupta, P. Dollar, and R. Girshick, "Lvis: A dataset for large vocabulary instance segmentation," in *Proceedings of the IEEE/CVF conference on computer vision and pattern recognition*, Conference Proceedings, pp. 5356–5364.

[22] R. Krishna, Y. Zhu, O. Groth, J. Johnson, K. Hata, J. Kravitz, S. Chen, Y. Kalantidis, L.-J. Li, and D. A. Shamma, "Visual genome: Connecting language and vision using crowdsourced dense image annotations," *International journal of computer vision*, vol. 123, pp. 32–73, 2017.

[23] T.-Y. Lin, M. Maire, S. J. Belongie, J. Hays, P. Perona, D. Ramanan, P. Dollár, and C. L. Zitnick, "Microsoft coco: Common objects in context," in *European Conference on Computer Vision*, Conference Proceedings.

[24] X. Chen, H. Fang, T.-Y. Lin, R. Vedantam, S. Gupta, P. Dollár, and C. L. Zitnick, "Microsoft coco captions: Data collection and evaluation server," *arXiv preprint arXiv:1504.00325*, 2015.

[25] P. Sharma, N. Ding, S. Goodman, and R. Soricut, "Conceptual captions: A cleaned, hypernymed, image alt-text dataset for automatic image captioning," in *Proceedings of the 56th Annual Meeting of the Association for Computational Linguistics (Volume 1: Long Papers)*, Conference Proceedings, pp. 2556–2565.

[26] B. A. Plummer, L. Wang, C. M. Cervantes, J. C. Caicedo, J. Hockenmaier, and S. Lazebnik, "Flickr30k entities: Collecting region-to-phrase correspondences for richer image-to-sentence models," in *Proceedings of the IEEE international conference on computer vision*, Conference Proceedings, pp. 2641–2649.

[27] M. Yuksekgonul, F. Bianchi, P. Kalluri, D. Jurafsky, and J. Zou, "When and why vision-language models behave like bags-of-words, and what to do about it?" in *The Eleventh International Conference on Learning Representations*, Conference Proceedings.

[28] J. He, J.-N. Chen, S. Liu, A. Kortylewski, C. Yang, Y. Bai, and C. Wang, "Transfg: A transformer architecture for fine-grained recognition," *Proceedings of the AAAI Conference on Artificial Intelligence*, vol. 36, no. 1, pp. 852–860, 2022. [Online]. Available: https://dx.doi.org/10.1609/aaai.v36i1.19967

[29] J. Krause, H. L. Jin, J. C. Yang, and F. F. Li, "Fine-grained recognition without part annotations," *2015 Ieee Conference on Computer Vision and Pattern Recognition (Cvpr)*, pp. 5546–5555, 2015. [Online]. Available: ⟨GotoISI⟩://WOS:000387959205065

[30] X.-S. Wei, Y.-Z. Song, O. Mac Aodha, J. Wu, Y. Peng, J. Tang, J. Yang, and S. J. Belongie, "Fine-grained image analysis with deep learning: A survey," *IEEE Transactions on Pattern Analysis and Machine Intelligence*, vol. 44, pp. 8927–8948, 2021.

[31] N. Zhang, J. Donahue, R. Girshick, and T. Darrell, "Part-based r-cnns for fine-grained category detection," in *13th European Conference on Computer Vision (ECCV)*, ser. Lecture Notes in Computer Science, vol. 8689, 2014, Conference Proceedings, pp. 834–849. [Online]. Available: ⟨GotoISI⟩://WOS:000345524200048

[32] L. Yao, R. Pi, J. Han, X. Liang, H. Xu, W. Zhang, Z. Li, and D. Xu, "Detclipv3: Towards versatile generative open-vocabulary object detection," in *Proceedings of the IEEE/CVF Conference on Computer Vision and Pattern Recognition*, Conference Proceedings, pp. 27 391–27 401.

[33] A. Vaswani, N. Shazeer, N. Parmar, J. Uszkoreit, L. Jones, A. N. Gomez, L. Kaiser, and I. Polosukhin, "Attention is all you need," *Advances in Neural Information Processing Systems 30 (Nips 2017)*, vol. 30, 2017. [Online]. Available: ⟨GotoISI⟩://WOS:000452649406008

[34] Y. Zang, W. Li, K. Zhou, C. Huang, and C. C. Loy, "Open-vocabulary detr with conditional matching," in *European Conference on Computer Vision*. Springer, Conference Proceedings, pp. 106–122.

[35] S. Zhao, Z. Zhang, S. Schulter, L. Zhao, B. Vijay Kumar, A. Stathopoulos, M. Chandraker, and D. N. Metaxas, "Exploiting unlabeled data with vision and language models for object detection," in *European Conference on Computer Vision*. Springer, Conference Proceedings, pp. 159–175.

[36] H. Touvron, T. Lavril, G. Izacard, X. Martinet, M.-A. Lachaux, T. Lacroix, B. Rozière, N. Goyal, E. Hambro, and F. Azhar, "Llama: Open and efficient foundation language models," *arXiv preprint arXiv:2302.13971*, 2023.

[37] J. Devlin, M.-W. Chang, K. Lee, and K. Toutanova, "Bert: Pre-training of deep bidirectional transformers for language understanding," *arXiv preprint arXiv:1810.04805*, 2018.

[38] M. Apidianaki, "From word types to tokens and back: A survey of approaches to word meaning representation and interpretation," *Computational Linguistics*, vol. 49, no. 2, pp. 465–523, 2023.

[39] W. Zheng, G. Gong, J. Tian, S. Lu, R. Wang, Z. Yin, X. Li, and L. Yin, "Design of a modified transformer architecture based on relative position coding," *International Journal of Computational Intelligence Systems*, vol. 16, no. 1, p. 168, 2023.

[40] Y. Yao, P. Liu, T. Zhao, Q. Zhang, J. Liao, C. Fang, K. Lee, and Q. Wang, "How to evaluate the generalization of detection? a benchmark for comprehensive open-vocabulary detection," in *Proceedings of the AAAI Conference on Artificial Intelligence*, vol. 38, Conference Proceedings, pp. 6630–6638.

[41] K. He, G. Gkioxari, P. Dollár, and R. Girshick, "Mask r-cnn," in *Proceedings of the IEEE international conference on computer vision*, Conference Proceedings, pp. 2961–2969.

[42] S. Ren, K. He, R. Girshick, and J. Sun, "Faster r-cnn: Towards real-time object detection with region proposal networks," *Advances in neural information processing systems*, vol. 28, 2015.

[43] E. B. Zaken, S. Ravfogel, and Y. Goldberg, "Bitfit: Simple parameter-efficient fine-tuning for transformer-based masked language-models," *arXiv preprint arXiv:2106.10199*, 2021.